ELSEVIER

Journal of Alloys and Compounds 421 (2006) 109–116

Journal of ALLOYS AND COMPOUNDS

www.elsevier.com/locate/jallcom

An alternative method for analyzing the non-isothermal glass-crystal transformation kinetics Application to the crystallization of some alloys of Ge-Sb-Se and Sb-As-Se glassy systems

J. Vázquez *, D. García-G. Barreda, P.L. López-Alemany, P. Villares, R. Jiménez-Garay

Departamento de Física de la Materia Condensada, Facultad de Ciencias, Universidad de Cádiz, Apartado 40, 11510 Puerto Real, Cádiz, Spain

Received 16 August 2005; received in revised form 9 November 2005; accepted 12 November 2005
Available online 6 January 2006

Abstract

A method has been developed for analyzing the non-isothermal glass-crystal transformation kinetics in materials for which the nucleation process takes place early in the transformation and the nucleation frequency is zero thereafter, the condition of "site saturation". Under this condition the Johnson–Mehl–Avrami transformation rate equation can be rigorously applied at non-isothermal processes. Considering the assumptions of extended volume and random nucleation, a general expression of the fraction transformed as a function of time in isothermal crystallization processes has been obtained. The application of the quoted expression to non-isothermal transformations has been carried out under the above-mentioned condition of "site saturation". Thus, the alternative method developed, starting from Johnson–Mehl–Avrami equation, initially equals two values of the volume fraction transformed, corresponding to two constant heating rates in different times, to deduce the activation energy of the transformation. Next, the kinetic exponent is obtained combining two transformed fractions, corresponding to two different values of the time in a single-scan. The theoretical method developed has been applied to the crystallization kinetics of some semiconducting alloys, prepared in our laboratory, corresponding to the Ge-Sb-Se and Sb-As-Se glassy systems, and which fulfil the condition of "site saturation". The obtained values for the kinetic parameters satisfactorily agree with the calculated results by the non-isothermal technique of multiple-scan. This fact confirms the reliability and accuracy of the theoretical model developed.

Keywords: Amorphous materials; Liquid quenching; X-ray diffraction; Calorimetry; Thermal analysis

1. Introduction

Knowledge of amorphous materials is one of the most active fields of research in the physics of condensed matter today [1], although traditionally, solid state physics has meant crystal physics, and solidity and crystallinity have been considered as synonymous in texts on condensed matter. Therefore, the solid state research in recent years has played an important role in the study of solids that are not crystals, solids for which the arrangement of the atoms lacks the slightest vestige of long-range order. The great interest in these materials is largely due to their ever increasing applications in modern technology. Their possibilities in the immediate future are huge based on the characteristic properties such as electronic-excitation phenomena, chemical reactivity and inertia and superconductivity. Therefore, the advances that have been made in the physics and chemistry of the quoted materials, during the last 40 years, have been very appreciated within the research community. A strong theoretical and practical interest in the application of isothermal and non-isothermal experimental analysis techniques to the study of phase transformations has arisen in the last decades. In the isothermal regime [2,3] the glass samples are quickly heated up and held a temperature above glass transition temperature. In this regime, the glasses crystallize a constant temperature. However, in the non-isothermal regime [4–8] the glass samples are heated up at a fixed heating rate. Generally, an isothermal experiment takes longer time than a non-isothermal experiment, but isothermal experimental data can be interpreted by the well-established

* Corresponding author.
E-mail address: jose.vazquez@uca.es (J. Vázquez).

0925-8388/$ – see front matter © 2005 Elsevier B.V. All rights reserved.
doi:10.1016/j.jallcom.2005.11.025

Johnson–Mehl–Avrami (JMA) kinetic equation [9–12]. On the contrary, the non-isothermal experiments have as advantage, the rapidity that makes this type of experiments more attractive. The use of non-isothermal techniques to study solid-state transformations and to determine the kinetic parameters of the rate controlling processes has been increasingly widespread. Therefore, the utilization of the non-isothermal regime has produced a large number of mathematical treatments for analyzing thermal process data, the most of the quoted treatments are based on the JMA transformation rate equation [9–12]. In this work the conditions of applicability of the JMA transformation rate equation to non-isothermal crystallization are established. According to Henderson [13] the above-mentioned equation can only be rigorously applied to glass-crystal transformations under non-isothermal regime if the nucleation process takes place early in the transformation and the nucleation frequency is zero thereafter, which can be referred to as "site saturation" [14]. In this sense, the present work describes an alternative method, based on the JMA equation, for deducing the kinetic parameters of the glass-crystal transformation in materials which fulfil the condition of "site saturation" [14]. The quoted method initially equals two values of the volume fraction transformed, corresponding to two constant heating rates in different times, to deduce the activation energy of the transformation. Next, the kinetic exponent is obtained combining two transformed fractions, corresponding to two different values of the time in a single-scan. Moreover, the present paper applies the alternative method developed to the analysis of the crystallization kinetics of the semiconducting alloys: $Ge_{0.13}Sb_{0.23}Se_{0.64}$ (S1), $Ge_{0.08}Sb_{0.15}Se_{0.77}$ (S2) and $Sb_{0.12}As_{0.40}Se_{0.48}$ (S3), prepared in our laboratory, and which fulfil the condition of "site saturation", according to literature [15]. We have confirmed the quoted condition checking that the kinetic exponent, n, is maintained constant after the reheating for the three alloys analyzed, as it is described in literature [15]. Finally, the obtained values for the kinetic parameters by means of the alternative method are compared with the corresponding results calculated by the non-isothermal technique of multiple-scan, finding that the error between them for the less accurate parameter is less than 4.5%. This fact shows the reliability and accuracy of the alternative method developed.

2. Theoretical background

2.1. Deducing the volume fraction transformed

The theoretical basis for interpreting DTA or DSC results is provided by the formal theory of transformation kinetics [10–13,16,17]. This formal theory supposes that the crystal growth rate, in general, is anisotropic, and therefore, the volume of a region originating at time $t = \tau$ (τ being the nucleation period) is then

$$v_\tau = g\prod_i \int_\tau^t u_i(t')\,\mathrm{d}t' \tag{1}$$

where the expression $\prod_i \int_\tau^t u_i(t')\,\mathrm{d}t'$ condenses the product of the integrals corresponding to the values of the above quoted subscript i and g is a geometric factor, which depends on the dimensionality and shape of the crystal growth, and therefore its dimension equation can be expressed as

$[g] = [\mathrm{L}]^{3-i}$ [L] is the length

Defining an extended volume of transformed material and assuming spatially random nucleation [5,18,19], the elemental extended volume, $\mathrm{d}V_\mathrm{e}$, in terms of nucleation frequency per unit volume, $I_\mathrm{V}(\tau)$, is expressed as

$$\mathrm{d}V_\mathrm{e} = v_\tau I_\mathrm{V}(\tau)V\,\mathrm{d}\tau = gI_\mathrm{V}(\tau)V\left(\prod_i \int_\tau^t u_i(t')\,\mathrm{d}t'\right)\mathrm{d}\tau \tag{2}$$

where V is the volume of the whole assembly.

The extended volume can be visualized as a series of volume elements having the same limiting surface as the actual transformed volume, V_b, but all growing 'through' each other. Some elements of the transformed volume are counted twice, others three times, and so on, in order to obtain the extended volume. It is possible now to find a relation between V_e and V_b. Consider any small random region, of which a fraction $(1 - V_\mathrm{b}/V)$ remains untransformed at time t. During a further time $\mathrm{d}t$, the extended volume will increase by $\mathrm{d}V_\mathrm{e}$, and the true volume by $\mathrm{d}V_\mathrm{b}$. Of the new elements of volume which make up $\mathrm{d}V_\mathrm{e}$, a fraction $(1 - V_\mathrm{b}/V)$ on average will lie in the previously untransformed material, and thus contribute to $\mathrm{d}V_\mathrm{b}$, whilst the remainder of $\mathrm{d}V_\mathrm{e}$ will be in the already transformed material. This result clearly follows only if $\mathrm{d}V_\mathrm{e}$ can be treated as a completely random volume element. Bearing in mind the hypothesis of random nucleation it is possible to write the relation between V_b and V_e in the form

$$\mathrm{d}V_\mathrm{b} = \left(1 - \frac{V_\mathrm{b}}{V}\right)\mathrm{d}V_\mathrm{e} = (1 - x)\,\mathrm{d}V_\mathrm{e} \tag{3}$$

where $x = V_\mathrm{b}/V$ is the volume fraction transformed. Differentiating this expression and substituting the result into Eq. (3), one obtains

$$\mathrm{d}V_\mathrm{e} = V\frac{\mathrm{d}x}{1 - x} \tag{4}$$

This equation is combined with Eq. (2) after the value for v_τ from Eq. (1) has been included, resulting in

$$\frac{\mathrm{d}x}{1 - x} = gI_\mathrm{V}(\tau)\left[\prod_i \int_\tau^t u_i(t')\,\mathrm{d}t'\right]\mathrm{d}\tau. \tag{5}$$

When the crystal growth rate is isotropic, $u_\mathrm{i} = u$, an assumption which is agreement with the experimental evidence, since in many transformations the reaction product grows approximately as spherical nodules [20], Eq. (5) can be written as

$$\frac{\mathrm{d}x}{1 - x} = gI_\mathrm{V}(\tau)\left(\int_\tau^t u(t')\,\mathrm{d}t'\right)^m \mathrm{d}\tau \tag{6}$$

where m is an exponent related to the dimensionality of the crystal growth and the mode of the transformation.

For the important case of isothermal transformation with nucleation frequency and growth rate independent of time, Eq.

(6) can be integrated to yield

$$x(t) = 1 - \exp\left[-gI_V u^m \int_0^t (t-\tau)^m \, d\tau\right]$$
$$= 1 - \exp(-g' I_V u^m t^n) \quad (7)$$

where $n = m + 1$ for $I_V \neq 0$ and g' is a new shape factor.

The last equation can be taken as a detailed specific case of the JMA relationship

$$x(t) = 1 - \exp[-(Kt)^n] \quad (8)$$

Here K is defined as the effective overall reaction rate constant, which is usually assigned an Arrhenian temperature dependence:

$$K = K_0 \exp\left(\frac{-E}{RT}\right) \quad (9)$$

where E is the effective activation energy, describing the overall transformation process and K_0 the frequency factor. It should be observed that K^n is proportional to $I_V u^m$. Hence assumption of an Arrhenian temperature dependence for K is appropriate when I_V and u vary in an Arrhenian manner with the temperature.

In general, the temperature dependence of the nucleation frequency is far from Arrhenian, and the temperature dependence of the crystal growth rate is also not Arrhenian when a broad range of temperature is considered [19]. Over a sufficiently limited range of temperature (such as the range of transformation peaks in DTA or DSC experiments), both I_V and u may be described in zeroth-order approximation by [21]

$$I_V \approx I_{V0} \exp\left(\frac{-E_N}{RT}\right) \quad (10)$$

and

$$u \approx u_0 \exp\left(\frac{-E_G}{RT}\right) \quad (11)$$

where E_N and E_G are the effective activation energies for nucleation and growth, respectively.

Combining Eqs. (7)–(11) one obtains

$$K_0^n \exp\left(\frac{-nE}{RT}\right) \propto I_{V0} u_0^m \exp\left[\frac{-(E_N + mE_G)}{RT}\right] \quad (12)$$

and the overall effective activation energy for the transformation is expressed as

$$E = \frac{E_N + mE_G}{n} \quad (13)$$

Eqs. (8) and (9) have served as the basis of nearly all treatments of transformation in DTA or DSC experiments. It should be noted, however, that Eq. (8) is strictly applied only to isothermal experiments, where an integration of the general expression of Eq. (6) is straightforward. In this case, the transformation rate, dx/dt, can be easily determined from Eq. (8) taking the derivative with respect to time and considering in the resulting expression the explicit relation between x and t given by Eq. (8), to yield

$$\frac{dx}{dt} = nK(1-x)[-\ln(1-x)]^{(n-1)/n}. \quad (14)$$

This equation is sometimes referred to as the JMA transformation rate equation.

2.2. An alternative method for deducing the kinetic parameters in materials which fulfil the Johnson–Mehl–Avrami transformation rate equation under non-isothermal regime

It was suggested by Henderson [13] in a notable paper that Eq. (14) as developed by Johnson, Mehl and Avrami is based on the following important assumptions:

1. isothermal transformation conditions;
2. spatially random nucleation;
3. growth rate of new phase dependent only on temperature and not time.

In the past decades Eq. (14) has been applied without qualification to the analysis of non-isothermal phase transformations [22–24]. However, according to literature [25], the above-mentioned equation can be rigorously applied under non-isothermal conditions if it can be shown that the transformation rate depends only on the state variables x and T. Under this restriction, according to literature [13], an example of a system which allows the non-isothermal application of Eq. (14) is one in which the nucleation process takes place early in the transformation and the nucleation frequency is zero thereafter, which can be referred to as "site saturation" [14]. Under this assumption it is possible to deduce the kinetic parameters, activation energy, E, kinetic exponent, n, and frequency factor, K_0, of a glass-crystal transformation from Eq. (8). In opposition to the methods which obtain the kinetic parameters from data based on the maximum value of the thermogram [26,27], the method, which is developed in this work, allows to use a large number of values obtained from the complete experimental curve for each of the different heating rates.

From Eq. (8) it is possible to consider two equal values of the volume fraction transformed, $x(t_i)$, corresponding to two exotherms taken at two constant heating rates, β_i, $(i = 1, 2)$, and bearing in mind Eq. (9), one obtains

$$\exp\left[\frac{E}{R}\left(\frac{1}{T_2} - \frac{1}{T_1}\right)\right] = \frac{t_2}{t_1} \quad (15)$$

where T_1 and T_2 are the temperatures corresponding to the equal values of the fraction transformed at the heating rates, β_i, and t_1, t_2 the corresponding effective times (transformation times minus incubation times).

Taking into account that $T_i = T_{0i} + \beta_i t_i$, where T_{0i} is the temperature at which the transformation at β_i begins, introducing into Eq. (15) the explicit forms of t_1 and t_2 given by the last expression and taking logarithm of the resulting equation, the results is the following expression

$$E = \frac{RT_1T_2}{T_1 - T_2} \ln\frac{(T_2 - T_{02})\beta_1}{(T_1 - T_{01})\beta_2} \quad (16)$$

for the effective activation energy of a non-isothermal glass-crystal transformation which fulfils the above-mentioned

assumptions. The last equation allows to calculate the kinetic parameter, E, for a set of fractions transformed, $x(t)$, and the corresponding mean value, represents the overall effective activation energy of the transformation.

Once the E-expression has been obtained, the kinetic exponent, n, can be deduced by using a single-scan $x(t_i)$, obtained at either heating rates, β_i, above considered. Assuming that Eq. (8) is valid for any t-value it is possible to write the volume fraction transformed for two values of time, namely

$$x(t_1) = 1 - \exp[-(K_1 t_1)^n] \tag{17}$$

and

$$x(t_2) = 1 - \exp[-(K_2 t_2)^n] \tag{18}$$

Combinig the logarithmic forms of Eqs. (17) and (18), and introducing into the resulting equation the K_i-expression, given by Eq. (9), one obtains

$$\frac{\ln[1 - x(t_1)]}{\ln[1 - x(t_2)]} = \left[\frac{t_1}{t_2}\ \exp\frac{E(T_1 - T_2)}{RT_1T_2}\right]^n \tag{19}$$

Taking logarithm of Eq. (19) and bearing in mind that for the same β it is verified $T_j = T_0 + \beta t_j$ ($j = 1, 2$) results in

$$n = \left\{\ln\frac{\ln[1 - x(t_1)]}{\ln[1 - x(t_2)]}\right\}\left[\frac{E(T_1 - T_2)}{RT_1T_2} + \ln\frac{T_1 - T_0}{T_2 - T_0}\right]^{-1} \tag{20}$$

an expression for the kinetic exponent, which allows to obtain the quoted exponent for the different values of the activation energy. The corresponding mean value may be considered as the most probable value of the kinetic exponent of the glass-crystal transformation.

Finally, after the parameters E and n have been determined, the frequency factor, K_0, related to the probability of effective molecular collisions for the formation of the activated complex, can be obtained from Eq. (17), yielding

$$K_0 = \frac{\beta\{-\ln[1 - x(t_1)]\}^{1/n}}{(T_1 - T_0)\ \exp(-E/RT_1)}. \tag{21}$$

3. Experimental details

In this section, the preparation of the glassy alloy (S1) is described as an illustrative example of the alloys analyzed in the present work and obtained in our laboratory. The semiconducting $Ge_{0.13}Sb_{0.23}Se_{0.64}$ glass was made in bulk form, from their components of 99.999% purity, which were pulverized to less than 64 μm, mixed in adequate proportions, and introduced into quartz ampoules. The ampoules were subjected to an alternating process of filling and vacuuming of inert gas, in order to ensure the absence of oxygen inside. This ended with a final vacuuming process of up to 10^{-2} Pa, and sealing with an oxyacetylene burner. The ampoules were put into a furnace at 1223 K for 44 h, turning at 1/3 rpm, in order to ensure the homogeneity of the molten material, and then quenched in water with ice to avoid the crystallization. The capsules containing the samples were then put into a mixture of hydrofluoridic acid and hydrogen peroxide in order to corrode the quartz and make it easier to extract the alloy. The glassy state of the material was confirmed by a diffractometric X-ray scan, in a Siemens D500 diffractometer, showing an absence of the peaks which are characteristic of crystalline phases. The homogeneity and composition of the samples were verified through scanning electron microscopy (SEM) in a Jeol, scanning microscope JSM-820. The calorimetric measurements were carried out in a Perkin-Elmer DSC7 differential scanning calorimeter with an accuracy of ±0.1 K. A constant 60 ml min^{-1} flow of nitrogen was maintained in order to provide a constant thermal blanket within the DSC cell, thus eliminating thermal gradients and ensuring the validity of the applied calibration standard from sample to sample. The calorimeter was calibrated, for each heating rate, using the well-known melting temperatures and melting enthalpies of high purity zinc and indium supplied with the instrument. The analyzed samples, were crimped into aluminium pans, and their masses were kept about 20 mg. An empty aluminium pan was used as reference. The crystallization experiments were carried out through continuous heating at rates, β, of 2, 4, 8, 16, 32 and 64 K min^{-1}. The glass transition temperature was considered as a temperature corresponding to the inflection point of the lambda-like trace on the DSC scan, as shown in Fig. 1. The crystallized fraction, x, at any temperature, T, is given by $x = A_T/A$, where A is the total area limited by the exotherm, between the temperature T_i where the crystallization is just beginning, and the temperature T_f where the crystallization is completed and A_T is the area between the initial temperature and a generic temperature T, see Fig. 1.

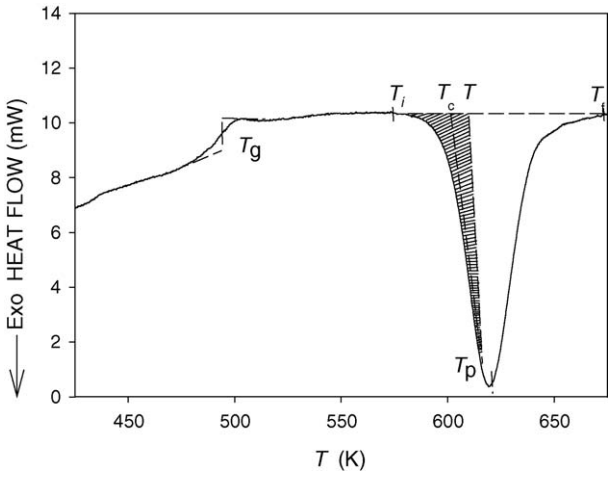

Fig. 1. Typical DSC trace of $Ge_{0.13}Sb_{0.23}Se_{0.64}$ glassy alloy at a heating rate of 32 K min^{-1}. The hatched area shows A_T, the area between T_i and T.

4. Results

Following with the alloy taken as an example, the typical DSC trace of chalcogenide $Ge_{0.13}Sb_{0.23}Se_{0.64}$ glass obtained at a heating rate of 32 K min^{-1} and plotted in Fig. 1, shows three characteristic phenomena, which are resolved in the temperature region studied. The first one ($T = 493$ K) correspond to the glass transition temperature, T_g, the second ($T = 601$ K) to the extrapolated onset crystallization temperature, T_c, and the third ($T = 619$ K) to the peak temperature of crystallization, T_p, of the above-mentioned chalcogenide glass. The quoted DSC trace shows the typical behaviour of a glass-crystal transformation. The thermograms for the different heating rates, β, quoted in Section 3, show values of the quantities T_g, T_c and T_p which increase with increasing β, a property which has been widely quoted in literature [27,28].

4.1. Glass-crystal transformation

The analysis of the crystallization kinetics is related to the knowledge of the reaction rate constant as a function of the temperature. This temperature dependence can be considered of Arrhenius type when a sufficiently limited range of temperature is used (such as the range of transformation peaks in DSC experiments). In order for this condition to hold, according to lit-

Table 1
Characteristic temperatures and enthalpies of the crystallization processes of the studied alloys

Parameter	Experimental value		
	S1	S2	S3
T_g (K)	474.0–499.2	414.4–433.1	459.2–490.9
T_i (K)	558.7–599.7	508.5–521.8	553.7–598.8
T_p (K)	581.1–631.3	529.0–572.8	579.2–641.4
ΔT (K)	42.0–56.7	34.5–79.8	51.1–73.0
ΔH (mcal mg^{-1})	6.2–7.7	5.3–6.4	4.1–5.1

erature [19], one of the following two sets of hypotheses should apply:

(i) The crystal growth rate, u, has an Arrhenian temperature dependence; and over the temperature range where the thermoanalytical measurements are carried out, the nucleation rate is negligible (i.e., the condition of "site saturation") [14].
(ii) Both the crystal growth and the nucleation, which have Arrhenian temperature dependences, occur simultaneously [6].

In the present work the first set of conditions is assumed in order to apply the JMA equation under regime of continuous heating. From this point of view, the crystallization kinetics of the alloys quoted in Section 1 has been analyzed by using the alternative method described in Section 2.2.

With the aim of analyzing the above-mentioned kinetics, the variation intervals of the quantities described by the thermograms of the alloys considered for the different heating rates, quoted in Section 3, are given in Table 1, where T_i and T_p are the temperatures at which crystallization begins and that corresponding to the maximum crystallization rate, respectively, and ΔT is the width of the peak. The crystallization enthalpy, ΔH, is also determined for each heating rate and each alloy.

The area under the DSC curve is directly proportional to the total amount of material transformed. The ratio between the ordinates and the total area of the peak gives the corresponding transformation rates, which allow to plot the curves of the exothermal peaks represented in Fig. 2 for the S1 alloy. It may be observed that the $(dx/dt)|_p$ values increase in the same proportion as the heating rate, a property which has been widely discussed in literature [27,28].

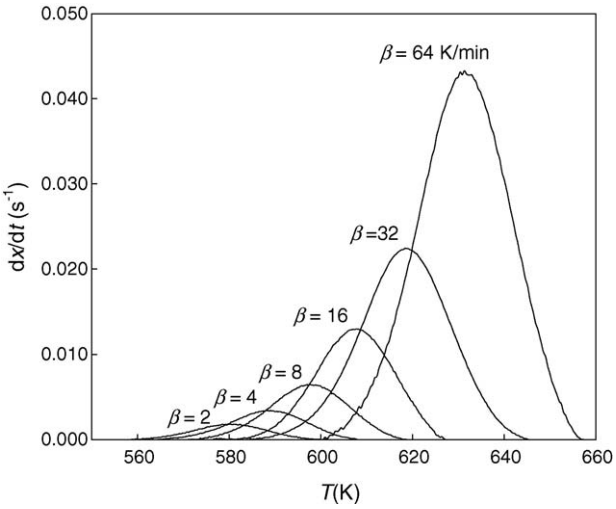

Fig. 2. Crystallization rate vs. temperature of the exothermal peaks, at different heating rates.

With the aim of correctly applying the preceding theory, the experimental temperatures T_1 and T_2, corresponding to the heating rates, β, 4 and 8 K min^{-1}, respectively, have been taken for equal transformed fractions, x, in the interval 0.2–0.8, with $\Delta x = 0.1$, as it is observed in Table 2. Also the initial temperatures of the transformation, T_{0i} ($i = 1, 2$), for each β_i quoted, are given in Table 2. It is interesting to denote that the JMA equation is more correctly fulfilled in the above quoted interval. From the experimental data quoted and using Eq. (16) the values of the activation energy, E, of the transformation are obtained for each transformed fraction and for each alloy, values which appear in Table 2. Next, according to the theoretical section, we have taken two experimental values of the fraction transformed, x_1 and x_2, and the corresponding temperatures T_1 and T_2, respectively, for a value of the heating rate, $\beta = 8$ K min^{-1}, besides the initial temperature, T_0, of the transformation for each alloy, as it can be observed in Table 3. From the quoted values and the activation energies shown in Table 2, using Eqs. (20) and (21), the values of the kinetic exponent, n, and of the frequency factor, K_0, are obtained and given in Table 3 for the analyzed alloys. It should be noted that with the aim of maintaining the simplicity,

Table 2
Experimental data and E-values for the analyzed alloys, obtained using the theoretical method developed

x	S1			S2			S3		
	T_1 (K)	T_2 (K)	E (cal mol^{-1})	T_1 (K)	T_2 (K)	E (cal mol^{-1})	T_1 (K)	T_2 (K)	E (cal mol^{-1})
0.0	564.5	571.6		508.0	514.0		562.6	577.6	
0.2	581.5	590.2	47590	529.1	536.6	47279	580.4	594.0	39295
0.3	584.1	592.9	48009	532.1	539.8	46627	583.6	597.2	39063
0.4	586.3	595.2	48135	534.5	542.3	46632	586.4	600.0	39001
0.5	588.5	597.6	47389	536.7	544.6	46547	589.2	602.8	39028
0.6	590.5	599.6	48171	539.0	546.9	47289	592.2	605.7	39597
0.7	592.6	601.9	47387	541.2	549.2	47159	595.3	608.9	39281
0.8	595.1	604.5	47506	543.7	551.8	47112	599.4	613.1	39116

Table 3
Kinetic parameters n and K_0 for the studied alloys, obtained using Eqs. (20) and (21), the corresponding experimental data and the E-values given in Table 2

S1			S2			S3		
Experimental data	n	K_0 ($\times 10^{-14}$ s^{-1})	Experimental data	n	K_0 ($\times 10^{-16}$ s^{-1})	Experimental data	n	K_0 ($\times 10^{-11}$ s^{-1})
$\beta = 8$ K min^{-1}	1.88	9.09	$\beta = 8$ K min^{-1}	1.47	2.24	$\beta = 8$ K min^{-1}	1.94	6.85
$T_0 = 571.6$ K	1.87	12.90	$T_0 = 514.0$ K	1.48	1.23	$T_0 = 577.6$ K	1.94	5.64
$T_1 = 592.2$ K	1.87	14.35	$T_1 = 539.6$ K	1.48	1.24	$T_1 = 596.9$ K	1.95	5.38
$T_2 = 597.8$ K	1.89	7.70	$T_2 = 546.5$ K	1.48	1.14	$T_2 = 603.0$ K	1.95	5.50
$x_1 = 0.2363$	1.87	14.79	$x_1 = 0.2325$	1.46	2.25	$x_1 = 0.2316$	1.93	8.80
$x_2 = 0.5776$	1.89	7.69	$x_2 = 0.5701$	1.47	2.00	$x_2 = 0.5748$	1.94	6.77
	1.89	8.50		1.47	1.92		1.94	5.90

Table 4
Mean values of the kinetic parameters for three glassy alloys

Alloy	$\langle E \rangle$ (cal mol^{-1})	$\langle n \rangle$	$\langle K_0 \rangle$ (s^{-1})
S1	47741	1.88	1.07×10^{15}
S2	46949	1.47	1.72×10^{16}
S3	39197	1.94	6.41×10^{11}

we have only used two fixed values of the fraction transformed, belonging to the heating rate of 8 K min^{-1}, to obtain the values of the kinetic parameters n and K_0. However, any other pair of x-values in the interval 0.2–0.8 gives a good result and the corresponding data for the heating rate of 4 K min^{-1} may be used with the same degree of accuracy.

Bearing in mind that the calorimetric analysis is an indirect method which makes it possible to obtain mean values for the parameters that control the kinetics of a reaction, the corresponding mean values of the kinetic parameters: E, n and K_0 are calculated and given in Table 4 for the three alloys analyzed. Once the quoted mean values have been obtained, the JMA equation can be written for each alloy. Combining Eqs. (8) and (9) and taking into account that $T = T_0 + \beta t$, it results in

$$x = 1 - \exp\left\{-[K_0(T - T_0)\beta^{-1}]^n \exp\left(\frac{-nE}{RT}\right)\right\} \quad (22)$$

and considering the mean values given in Table 4, the expressions of the theoretical fraction transformed are obtained and given in Table 5 for each alloy and for the heating rates of 16 and 32 K min^{-1}. It should be noted that the quoted heating rates are different to those used to obtain the kinetic parameters by the alternative method, thus allowing to test the reliability of the described procedure. As an illustrative example, the theoretical and experimental curves x versus T for the S1 alloy and

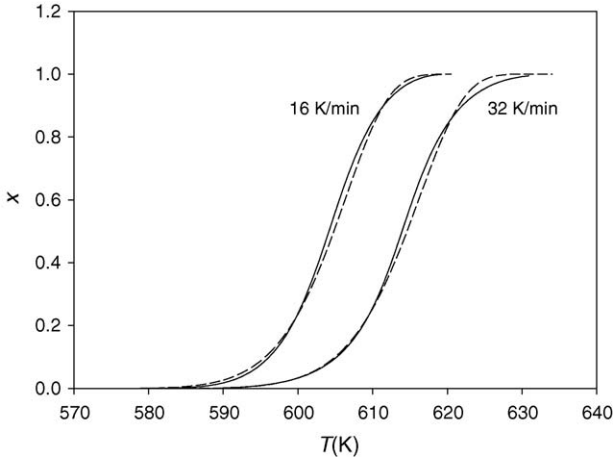

Fig. 3. Crystallized fraction, x, vs. temperature, T, for the heating rates of 16 and 32 K min^{-1} in the case of S1 alloy. Continuous line experimental curve, broken line theoretical curve.

for the above quoted heating rates are represented in Fig. 3. It is observed a very satisfactory agreement between both curves, which confirms the validity of the theoretical method described.

On the other hand, the multiple-scan technique, which allows E to be quickly evaluated, has been used to analyze the crystallization kinetics of the three semiconducting alloys considered. In the quoted technique, according to literature [29], the following equations

$$\ln\left(\frac{T_p^2}{\beta}\right) = \frac{E}{RT_p} - \ln\frac{RK_0}{E} \quad (23)$$

and

$$n = \left(\frac{dx}{dt}\right)|_p RT_p^2(0.37\beta E)^{-1} \quad (24)$$

Table 5
Theoretical expressions of the volume fraction transformed for the studied alloys

Alloy	β (K min^{-1})	JMA equation
S1	16	$x = 1 - \exp\{-[1.07 \times 10^{15} \times 3.75\,(T - 576.5)]^{1.88} \exp[-(1.88 \times 47741)\,(2T)^{-1}]\}$
	32	$x = 1 - \exp\{-[1.07 \times 10^{15} \times 1.875\,(T - 584.4)]^{1.88} \exp[-(1.88 \times 47741)\,(2T)^{-1}]\}$
S2	16	$x = 1 - \exp\{-[1.72 \times 10^{16} \times 3.75\,(T - 519.7)]^{1.47} \exp[-(1.47 \times 46949)\,(2T)^{-1}]\}$
	32	$x = 1 - \exp\{-[1.72 \times 10^{16} \times 1.875\,(T - 520.9)]^{1.47} \exp[-(1.47 \times 46949)\,(2T)^{-1}]\}$
S3	16	$x = 1 - \exp\{-[6.41 \times 10^{11} \times 3.75\,(T - 579.1)]^{1.94} \exp[-(1.94 \times 39197)\,(2T)^{-1}]\}$
	32	$x = 1 - \exp\{-[6.41 \times 10^{11} \times 1.875\,(T - 590.1)]^{1.94} \exp[-(1.94 \times 39197)\,(2T)^{-1}]\}$

Table 6
Kinetic parameters obtained for the crystallization of the S1 alloy using the multiple-scan technique

β (K min^{-1})	T_p (K)	$(dx/dt)\|_p$ ($\times 10^3$ s^{-1})	n	$\langle n \rangle$	E (cal mol^{-1})	K_0 (s^{-1})
2	581.1	1.81	2.08			
4	588.0	3.42	2.01			
8	597.5	6.45	1.96	1.96	47863	1.81×10^{15}
16	607.7	12.99	2.04			
32	618.3	22.44	1.82			
64	631.3	43.28	1.83			

allow to obtain the kinetic parameters, by using the experimental data: maximum transformation rate, $(dx/dt)|_p$, and corresponding temperature, T_p, to each heating rate. Thus, the activation energy and the frequency factor are obtained from the slope and intercept of Eq. (23), respectively, and the kinetic exponent from Eq. (24). As an example of the application of the multiple-scan technique we put forward the case of S1 alloy. In this sense, the experimental values of the quantities T_p and $(dx/dt)|_p$ for the different heating rates, together with the calculated values for the kinetic parameters are given in Table 6. The plots of $\ln(T_p^2/\beta)$ versus $1/T_p$ for each heating rate, and the straight regression line carried out for the S1 alloy are shown in Fig. 4. The kinetic parameters of the alloys S2 and S3 have been obtained of similar form by means of the multiple-scan technique.

With the aim of correctly analyzing the reliability of the theoretical method described, when calculating kinetic parameters in non-isothermal crystallization processes under the condition of "site saturation" [14,26], the above-mentioned parameters E, n and $\ln K_0$, calculated by means of the quoted theoretical method, are compared with its values obtained through the multiple-scan technique, Table 7, finding that the error between them for the less accurate parameter is less than 4.5%. This result is in agreement with literature [24], where it is shown that for $(n-1)/n = 0.6$ in the range of $0.2 < x < 0.7$ it results in an error of 7% in the calculated slope, E/R, an error acceptable in most crystallization reactions. The quoted fact also confirms that the theoretical method developed is adequate to describe the crystallization kinetics of the glassy alloys, which fulfil the condition of "site saturation".

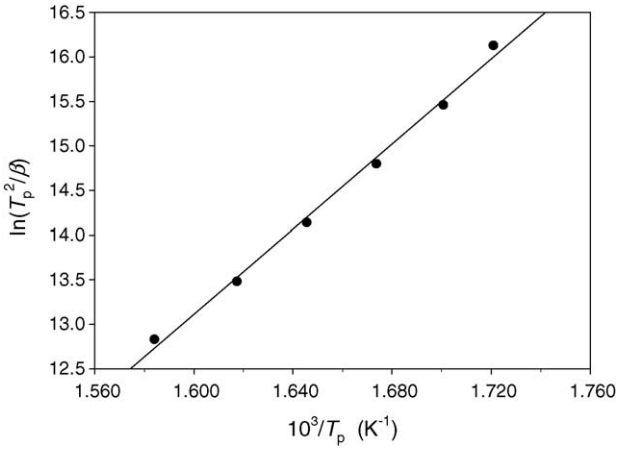

Fig. 4. Plots of $\ln(T_p^2/\beta)$ vs. $1/T_p$ and straight regression line of the $Ge_{0.13}Sb_{0.23}Se_{0.64}$ alloy (β in K s^{-1}).

Table 7
Kinetic parameters calculated by the alternative method described in Section 2.2 and by the multiple-scan technique

Alloy	Method	E (cal mol^{-1})	n	$\ln K_0$
S1	Object of this work	47741	1.88	34.60
	Multiple-scan	47863	1.96	35.13
S2	Object of this work	46949	1.47	37.38
	Multiple-scan	47000	1.45	37.77
S3	Object of this work	39197	1.94	27.19
	Multiple-scan	37545	1.90	27.15

5. Conclusions

The alternative method described enables us to study the crystallization kinetics in materials involving nucleation and crystal growth processes, which occur in separate stages. This method assumes the concept of extended volume in the transformed material and the condition of random nucleation. Using these assumptions a general expression for the transformed fraction as a function of time in bulk crystallization has been obtained. In the case of isothermal crystallization, the above-mentioned expression has been transformed in an equation which can be taken as a specific case of the JMA transformation equation. The application of this equation to non-isothermal transformations implies that the nucleation process takes place early in the transformation and the nucleation frequency is zero thereafter, condition of "site saturation". Under this restriction, the alternative method developed obtains the kinetic parameters of crystallization in a glassy system heated under non-isothermal regime. From JMA equation the kinetic parameters are deduced by means of two scans of DSC data recorded at two heating rates. The quoted method initially obtains the activation energy by equalling two values of the volume fraction transformed, corresponding to two constant heating rates. Next, the kinetic exponent is deduced combining two transformed fractions, corresponding to two different values of the time in a single-scan. The alternative method has been applied to the crystallization kinetics of some glassy alloys, prepared in our laboratory, which fulfil the condition of "site saturation". The quoted alloys have been also analyzed by means of the multiple-scan technique, finding that the error between the values of the kinetic parameters obtained by both methods is less than 4.5%. This good agreement shows the reliability of the alternative method developed for the calculation of the kinetic parameters in materials involving

nucleation and crystal growth processes, which occur in separate stages.

Acknowledgments

The authors are grateful to the Junta de Andalucía and Comisión Interministerial de Ciencia y Tecnología (CICYT, project no. MAT 2001-3333) for their financial supports.

References

[1] R. Zallen, The Physics of Amorphous Solids, Wiley, New York, 1983.
[2] J.Q. Zhu, Z.L. Bo, D.K. Dong, Phys. Chem. Glasses 37 (1996) 264.
[3] M.A. Abdel-Rahim, M.M. Ibrahim, M. Dongol, A. Gaber, J. Mater. Sci. 27 (1992) 4685.
[4] M.C. Weinberg, R. Kapral, J. Chem. Phys. 91 (1989) 7146.
[5] J. Vázquez, P. Villares, R. Jiménez-Garay, J. Alloys Compd. 257 (1997) 259.
[6] J.R. Frade, J. Am. Ceram. Soc. 81 (1998) 2654.
[7] C.S. Ray, X. Fang, D.E. Day, J. Am. Ceram. Soc. 83 (2000) 865.
[8] P.L. López-Alemany, J. Vázquez, P. Villares, R. Jiménez-Garay, Mater. Lett. 57 (2003) 2722.
[9] W.A. Johnson, K.F. Mehl, Trans. Am. Inst. Mining Met. Eng. 135 (1939) 416.
[10] M. Avrami, J. Chem. Phys. 7 (1939) 1103.
[11] M. Avrami, J. Chem. Phys. 8 (1940) 212.
[12] M. Avrami, J. Chem. Phys. 9 (1941) 177.
[13] D.W. Henderson, J. Non-Cryst. Solids 30 (1979) 301.
[14] J.W. Cahn, Acta Metall. 4 (1956) 572;
J.W. Cahn, Acta Metall. 4 (1956) 449.
[15] K. Matusita, T. Komatsu, R. Yokota, J. Mater. Sci. 19 (1984) 291.
[16] A.N. Kolomogorov, Bull. Acad. Sci. USSR (Sci. Mater. Nat.) 3 (1937) 3551.
[17] P.L. López-Alemany, J. Vázquez, P. Villares, R. Jiménez-Garay, J. Non-Cryst. Solids 274 (2000) 249.
[18] V.A. Shneidman, D.R. Uhlmann, J. Chem. Phys. 109 (1998) 186.
[19] H. Yinnon, D.R. Uhlmann, J. Non-Cryst. Solids 54 (1983) 253.
[20] J.W. Christian, The Theory of Transformations in Metals and Alloys, second ed., Pergamon Press, New York, 1975.
[21] S.O. Kasap, C. Juhasz, J. Chem. Soc. Faraday Trans. 2 (81) (1985) 811.
[22] F. Skvara, V. Satava, J. Therm. Anal. 2 (1970) 325.
[23] J. Sestak, Thermochim. Acta 3 (1971) 1.
[24] J. Sestak, Phys. Chem. Glasses 6 (1974) 137.
[25] T. Kemény, Thermochim. Acta 110 (1987) 131.
[26] J.A. Augis, J.E. Bennett, J. Therm. Anal. 13 (1978) 283.
[27] Y.Q. Gao, W. Wang, J. Non-Cryst. Solids 81 (1986) 129.
[28] J. Vázquez, P.L. López-Alemany, P. Villares, R. Jiménez-Garay, Mater. Chem. Phys. 57 (1998) 162.
[29] J. Vázquez, P.L. López-Alemany, P. Villares, R. Jiménez-Garay, J. Alloys Compd. 270 (1998) 179.